Journal of Solid State Chemistry 184 (2011) 3319–3323

Contents lists available at SciVerse ScienceDirect

Journal of Solid State Chemistry

journal homepage: www.elsevier.com/locate/jssc

$CdCu_3(OH)_6Cl_2$: A new layered hydroxide chloride

T.M. McQueen [a,*], T.H. Han [b], D.E. Freedman [a], P.W. Stephens [c], Y.S. Lee [b], D.G. Nocera [a]

[a] Department of Chemistry, Massachusetts Institute of Technology, 77 Massachusetts Avenue, Cambridge, MA 02139-4307, United States
[b] Department of Physics, Massachusetts Institute of Technology, 77 Massachusetts Avenue, Cambridge, MA 02139-4307, United States
[c] Department of Physics and Astronomy, Stony Brook University, Stony Brook, NY 11794, United States

ARTICLE INFO

Article history:
Received 8 August 2011
Received in revised form
6 October 2011
Accepted 10 October 2011
Available online 25 October 2011

Keywords:
$CdCu_3(OH)_6Cl_2$
Herbertsmithite
Kapellasite
Pseudopolyatomic
Kagome
Paratacamite

ABSTRACT

A new transition metal hydroxide chloride containing kagomé layers of magnetic ions, $CdCu_3(OH)_6Cl_2$, has been synthesized and structurally characterized. The actual low symmetry $P2_1/n$ structure can be derived from the ideal trigonal one with a change in cation distribution and coherent distortions of the anion framework. The result is a fundamentally different Cu^{2+} kagomé framework than found in the related Herbertsmithite and Kapellasite minerals. Magnetization measurements show no transition to long range magnetic order above $T=2$ K, despite strong antiferromagnetic interactions with a Weiss temperature of $\theta_w=-150$ K. Furthermore, we show that the structure of $CdCu_3(OH)_6Cl_2$ and related hydroxide chlorides can be rationalized on the basis of $[(OH)_3Cl]^{4-}$ pseudopolyatomic anions that pack and rotate, in much the same way as do traditional polyatomic anions. This opens the door to rational design of new and useful hydroxide chloride materials.

1. Introduction

Layered transition metal hydroxide chlorides are common minerals known to exist in a wide variety of structural polymorphs [1–5]. They have come under intense scrutiny for their magnetic properties in recent years following the discovery that the synthetic version of the mineral Herbertsmithite, with nominal formula "$ZnCu_3(OH)_6Cl_2$," contains kagomé layers of Cu^{2+} and exhibits a high degree of geometric magnetic frustration and may possess an exotic spin liquid or valence bond solid electronic ground state [6–14]. Recent experiments on samples of nominal "$ZnCu_3(OH)_6Cl_2$," as well as studies of the isostructural Mg^{2+} analog, have shown that there is significant variability in the interlayer Cu/(Zn/Mg) cation composition of these synthetic materials, and that the true structural–chemical formulas should be written as $(A_xCu_{1-x})Cu_3(OH)_6Cl_2$ ($A=Zn^{2+}$, Mg^{2+}), with x ranging from 0 to an upper limit of 0.75 ($A=Mg^{2+}$) or 0.85 ($A=Zn^{2+}$) [15,16]. The Cu intralayer composition of the kagomé structure is not perturbed, however, and the electronic properties of synthetic $Zn_{0.85}Cu_{3.15}(OH)_6Cl_2$ is thought to arise from the properties of the material as a pinned spin liquid [17].

Here we report the synthesis and structural characterization of a related hydroxide chloride, $CdCu_3(OH)_6Cl_2$. It has the same basic anion arrangement as that found in the $ZnCu_3(OH)_6Cl_2$ family of materials, but with a significantly different cation distribution that derives from the large size of the Cd^{2+} ion (0.95 Å) [18]. This large size also causes displacements of the anions, resulting in a comparatively low-symmetry structure that contains magnetic Cu^{2+} (d^9) on a kagomé lattice. The material is a geometrically frustrated antiferromagnet, as evidenced by strong magnetic interactions with a Weiss temperature of $\theta_w=-150$ K, with no transition to long range magnetic order above 2 K in magnetization measurements. Further, We show that the structure of $CdCu_3(OH)_6Cl_2$ and related hydroxide chlorides can be understood in terms of rigid $[(OH)_3Cl]^{4-}$ pseudopolyatomic anions that pack and rotate, in much the same way as do traditional polyatomic ions such as SO_4^{2-} and PO_4^{3-}.

2. Experimental

$CdCu_3(OH)_6Cl_2$ was prepared hydrothermally at 130 °C. In a typical reaction, 1.5 g (8.2 mmol) of $CdCl_2$ (Sigma-Aldrich, 99+%, anhydrous; WARNING: toxic) was dissolved in 15 mL of deionized (> 18.2 MΩ-cm) H_2O. This solution was put in the Teflon liner of an acid digestion autoclave (Parr Instrument Co. #4749) and 0.48 g (5.0 mmol) of $Cu(OH)_2$ (NOAH Technologies, 99+%) was added. The reaction vessel was sealed and then heated to 130 °C at 30 °C/h, held at 130 °C for 2 day, and then cooled at 30 °C/h to

* Corresponding author. Current address: Department of Chemistry and Department of Physics and Astronomy, The Johns Hopkins University, Baltimore, MD 21218, United States.
E-mail address: mcqueen@jhu.edu (T.M. McQueen).

0022-4596/$ - see front matter © 2011 Elsevier Inc. All rights reserved.
doi:10.1016/j.jssc.2011.10.015

room temperature. The solution was filtered, and the bright blue precipitate washed with deionized H_2O 10 × and then dried in a $CaSO_4$ desiccator. Inductively Coupled Plasma Optical Emission Spectroscopy (ICP-OES) for metals analysis was performed using a HORIBA Jorbin ACTIVA spectrometer. Standards were prepared from materials purchased commercially from Sigma-Aldrich, designated as TraceSELECT grade or better. ICP-OES analysis gave a Cd:Cu ratio of 1:3.04(9). Synchrotron x-ray diffraction (SXRD) data were collected on the SUNY X16C beamline at the National Synchrotron Light Source using an incident wavelength of 0.69923 Å. Refinements of the SXRD data were carried out using GSAS with the EXPGUI interface. Magnetization measurements were performed from $T=2$ to 350 K using a quantum design magnetic properties measurement system using an applied magnetic field of $\mu_0H=1$ T.

3. Results

The synchrotron X-ray diffraction (SXRD) data for $CdCu_3(OH)_6Cl_2$ could be indexed with a rhombohedral unit cell, $a=6.9899(4)$ Å and $c=14.356(1)$ Å in the hexagonal setting. The atomic coordinates for Herbertsmithite-like $ZnCu_3(OH)_6Cl_2$ ($AB_3(OH)_6Cl_2$) were used as a starting model for Rietveld refinements, with Cd in place of Zn. However, no simple set of parameters within this model (including preferred orientation, absorption corrections, non-negative thermal parameters, Cu substitution for Cd on the A site, or variation of the O/Cl or metal/anion ratios) were able to reliably fit the data, with the worst agreement at the (003), (110) and (201) reflections, where this model mispredicts the observed intensity by a factor of 10 or more, as shown in the inset of Fig. 1. This implies that the atomic positions of Cd, the strongest X-ray scatterer by a factor of $48^2/29^2 \sim e$, are not correct. A reasonable fit was only obtained when Cd and Cu were allowed to mix, $(Cd_{1-y}Cu_y)(Cu_{3-x}Cd_x)(OH)_6Cl_2$. Free refinement of the relative Cd and Cu occupancies of the *A* and *B* sites (with all thermal parameters constrained to the same value) gave $y=0.89(1)$ and $x=0.90(2)$. Full parameters for this model are given in Table 1. While the total, freely refined Cd:Cu ratio is 1.01:3, which is consistent with the ICP-OES measurement, there is little occupancy of the *A* site with Cd, and random mixing of Cd and Cu on the *B* site. This random mixing of Cd and Cu is unexpected given the large difference in ionic size between Cd^{2+} (0.95 Å) and Cu^{2+} (0.73 Å) [18]. Instead, this suggests that the disordered trigonal model, with random mixing of Cd and Cu on the *B* site, is not correct.

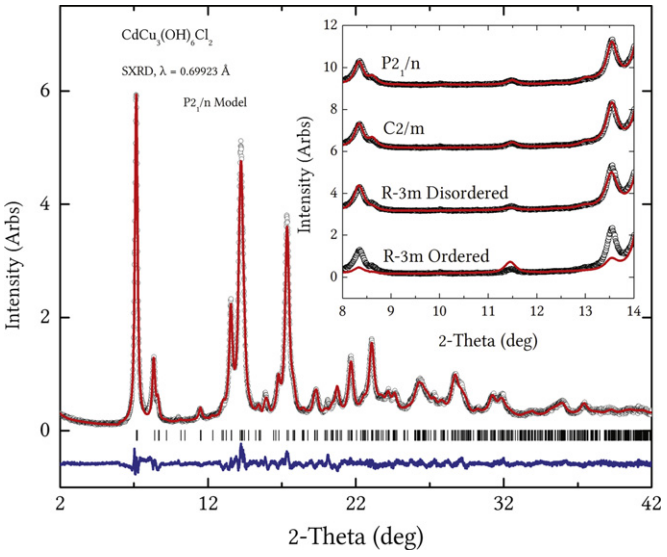

Fig. 1. Final Rietveld refinement of the SXRD data for $CdCu_3(OH)_6Cl_2$ using the $P2_1/n$ model. There are no systematic trends or errors in residual. The inset shows a region of the diffraction pattern, containing the trigonal (003), (110), and (201) reflections, with fits to the different structural models.

An improved model can be derived from the trigonal one with a structural distortion or supercell that splits the *B* site into multiple crystallographic sites. There are no visible low angle superstructure peaks, making a structural distortion, rather than supercell or loss of rhombohedral centering, more likely. We would expect to see the superstructure peaks due to the large difference in scattering factor between Cd and Cu. From supergroup–subgroup relations, the most likely possibilities are a monoclinic $C2/m$ distortion (as is seen in many $NaMO_2$ compounds, e.g., $NaVO_2$ [19,20]), or the lower symmetry monoclinic $P2_1/n$ distortion observed in $Cu_4(OH)_6Cl_2$ [21]. Either of these possibilities would not necessarily result in observable superstructure reflections.

In addition, either possibility also explains the rather broad nature of the peaks in the SXRD pattern. Fig. 2 shows the relationship between the structural core of the *R*-3*m*, *C*2/*m* and $P2_1/n$ models. In *R*-3*m*, there is only one kind of *A* site (with O_6 coordination) and one kind of *B* site (with O_4Cl_2 coordination), with all oxygen ions equivalent. The *C*2/*m* model breaks the *B* site into two crystallographic sites, *B*′ and *B*″ in a ratio of 2:1. As a consequence, the oxygen ions are also split across two sites. In this model, the Cd ions occupy the *B*″ site and Cu occupies the *B*′ and *A* sites. The $P2_1/n$ model is very similar to the *C*2/*m* one, but involves an extra rotation of the $B'O_4Cl_2$ octahedra (to engender a total of three oxygen sites). This allows for expansion of the $B''O_4Cl_2$ cavity, as might be expected given the large size of Cd^{2+}. The results of Rietveld refinements using the *C*2/*m* and $P2_1/n$ models is given in Table 1. Both models provide good fits to the data. The diffraction data is not of sufficient quality to conclusively discriminate between these two options, and attempts at convergent beam electron diffraction have been unsuccessful due to extreme sensitivity to the electron beam.

However, the $P2_1/n$ model gives more reasonable Cd–O bond lengths than the *C*2/*m* model because the $P2_1/n$ model allows for a slight rotation of the CuO_4Cl_2 octahedra to enlarge the CdO_4Cl_2 cavity. Furthermore, the title compound is chemically similar to $Cu_4(OH)_6Cl_2$, which is known to exist in the $P2_1/n$ space group [21]; applying a *t*-test suggests the $P2_1/n$ model is a significant improvement over the *C*2/*m* one at the 95% confidence level [22]. Additionally, inspection of the O–H stretch region of the IR spectrum of $CdCu_3(OH)_6Cl_2$ (not shown) shows the presence of three vibrational modes; the $P2_1/n$ structure is more consistent with this observation, since there are three crystallographically distinct O sites (and thus at least three possible O–H stretches), versus only two in the *C*2/*m* structure (which would produce only two O–H stretching modes unless the protons were disordered in the structure). Consequently, the $P2_1/n$ model is selected as the correct one for $CdCu_3(OH)_6Cl_2$. Allowing for changes in the Cd/Cu, O/Cl, or metal/anion ratios during the refinements in $P2_1/n$ did not result in a statistically significant improvement, and thus the assumed Cd:Cu:O:Cl ratio of 1:3:6:2 (consistent with the ICP-OES ratio of 1:3 for Cd:Cu) is taken to be correct. The final Rietveld refinement using $P2_1/n$ is shown in Fig. 1.

4. Discussion

Due to the low scattering power, it was not possible to directly locate the positions of the H atoms from the OH^- anions, but they must be present for charge balance. Their presence is indirectly indicated by the bond valence sums (BVS) around O1, O2, and O3.

Table 1
Unit cell and atomic position parameters for three different structural models for $CdCu_3(OH)_6Cl_2$.

Space group	$R\bar{3}m$[c]	$C2/m$[d]	$P2_1/n$[d]
a (Å)	6.9899(5)	12.151(2)	6.3048(8)
b (Å)		6.976(1)	6.979(1)
c (Å)	14.355(2)	6.306(1)	9.375(1)
β (deg.)		130.52(1)	99.73(1)
γ (deg.)	120		
A[a]	3*a* (0,0,0)	2*a* (0,0,0)	2*d* (0,½,½)
Cd/Cu occ.	0.13(1)/0.87(1)	0/1	0/1
B[b]	9*d* (1/3,1/6,1/6)		
Cd/Cu occ.	0.30(1)/0.70(1)		
B'(Cu)		4*f* (¼,¼,½)	4*e* (0.279(1),0.243(2),0.753(1))
B''(Cd)		2*c* (0,0,½)	2*a* (0,0,0)
Cl	6*c* (0,0,0.310(1))	4*i* (0.702(1),0,0.069(1))	4*e* (0.125(1),−0.022(2),0.300(1))
O1	18*h* (0.144(1),0.289(1),0.101(1))	4*i* (0.290(2),0,0.354(3))	4*e* (0.242(4),0.286(4),0.543(3))
O2		8*j* (0.031(1),0.203(2),0.253(2))	4*e* (0.433(4),−0.010(8),0.712(2))
O3			4*e* (0.204(4),0.700(4),0.522(4))
U_{iso}	0.0263(4)	0.0204(3)	0.0185(4)
χ^2	5.268	5.004	3.994
N_{var}/N_{obs}	24/188	38/359	55/624
R_{wp} (%)	7.61	7.40	6.60
R_p (%)	5.83	5.62	5.00
$R(F^2)$ (%)	4.95	3.59	2.62

[a] The "*A*" site has O_6 octahedral coordination.
[b] "*B*" sites have O_4Cl_2 coordination.
[c] A single thermal parameter was used for the R-3m model to allow for refining of the relative *A* and *B* site occupancies by Cd and Cu. The positions of the hydrogen atoms were not determined.
[d] For the $C2/m$ and $P2_1/n$ models, a single thermal parameter was used due to large correlations with some atomic positions. The positions of the hydrogen atoms were not determined by Rietveld refinement.

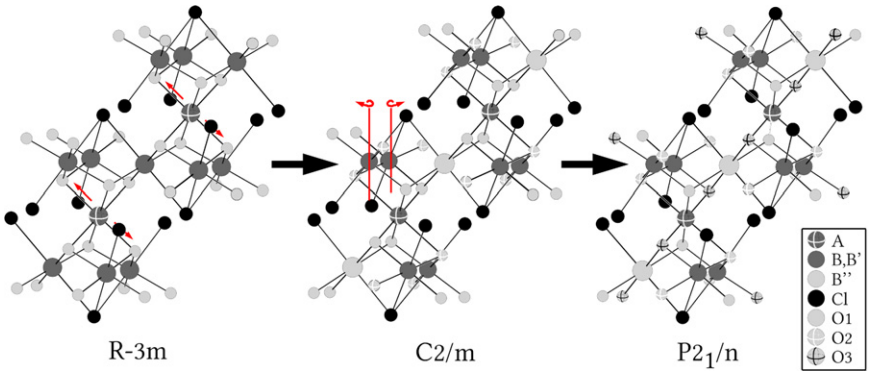

Fig. 2. The Cu^{2+} in O_6 coordination Jahn–Teller distortion and subsequent octahedral tilting to accommodate the large size of Cd^{2+} that relates the three structural models tested for $CdCu_3(OH)_6Cl_2$.

Without the H atoms to make OH^- anions, the BVS's are −1.1, −0.7, and −1.1 for O1, O2, and O3, respectively, significantly lower than the expected −2 for each. By analogy to the numerous isomorphic compounds in which the hydrogen atoms have been directly located [6,15], we place the H atoms 0.97 Å away from the O atoms, along the O–Cl vector. The result is BVS's of −2.1, −1.6, and −2.1 for O1, O2, and O3, respectively, in good agreement with the expected value of −2 for each. The final $P2_1/n$ structural model is shown in Fig. 3a.

The structure can be viewed as kagomé layers of $S=½$ Cu^{2+} ions that are separated by non-magnetic Cd^{2+} ions (Fig. 3b). The kagomé layers have two kinds of Cu sites, one coordinated by six oxygens, the other by four oxygens and two chlorines. As expected for d^9 Cu^{2+}, the coordination polyhedra of both Cu sites show strong tetragonal distortions. Cu1 has four Cu–O bond lengths ~2 Å, characteristic of a metal–oxygen bond, and two axial Cu–O bonds of length ~2.6 Å, which is essentially non-bonding. Similarly, Cu2 has four Cu–O bonds of length ~2 Å, and two axial Cu–Cl bonds of length ~2.9 Å. Separating these kagomé layers are layers of non-magnetic Cd^{2+} ions in O_4Cl_2 coordination. Also as expected, the Cd site has bond lengths characteristic of bonding to all six nearest neighbors: four Cd–O bonds of ~2.3 Å (vs. 2.35 Å as expected from ionic radii) and two Cd–Cl bonds of ~2.8 Å (vs. 2.76 Å as expected from ionic radii). These bond lengths are also comparable to those found in related hydroxide chlorides. Table 2 shows a comparison of salient bond lengths in $CdCu_3(OH)_6Cl_2$ to those found in the related compounds β-$Cd_2(OH)_3Cl$ and $Cu_2(OH)_3Cl$ [4,21,23].

The kagomé layers of Cu exhibit signs of geometric magnetic frustration. Fig. 4 shows the zero-field-cooled inverse magnetic susceptibility of $CdCu_3(OH)_6Cl_2$ calculated assuming $\chi = M/H$ using magnetization data collected under an applied magnetic field of $\mu_0H=1$ T, and after subtraction of a temperature-independent contribution of $\chi_0=8.5\times10^{-5}$ emu mol-Cu^{-1} Oe^{-1} to account for contributions from core diamagnetism and the sample holder. The sample follows Curie–Weiss behavior above

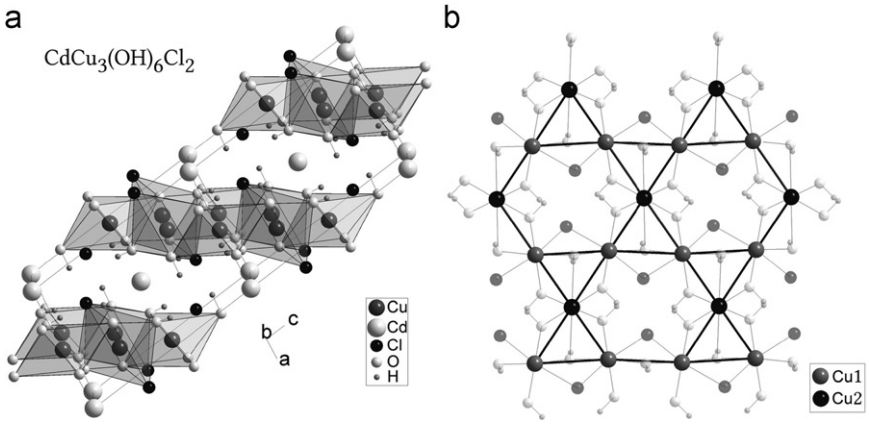

Fig. 3. (a) Final structural model for $CdCu_3(OH)_6Cl_2$, including placement of the H ions based on their positions in related structures. (b) $CdCu_3(OH)_6Cl_2$ contains kagomé layers of Cu^{2+} ions with two inequivalent sites that are separated by layers of Cd^{2+} ions.

Table 2
Comparison of metal–anion bond length parameters of $CdCu_3(OH)_6Cl_2$ to those found in related structures.

d[a]	β-$Cd_2(OH)_3Cl$	$Cu_2(OH)_3Cl$ *P*2_1/*n*	$CdCu_3(OH)_6Cl_2$ *P*2_1/*n*
Cd–O	2.2405 (× 2) 2.2450 (× 2)		2.30(3) (× 2) 2.37(3) (× 2)
Cd–Cl	2.8294 (× 2)		2.79(1) (× 2)
Cu_A–O		1.9110 (× 2) 1.9725 (× 2) 2.3699 (× 2)	1.88(2) (× 2) 2.12(3) (× 2) 2.66(3) (× 2)
Cu_B–O		1.897 (× 1) 1.949 (× 1) 2.021 (× 1) 2.076 (× 1)	1.97(3) (× 1) 2.08(5) (× 1) 2.12(4) (× 1) 2.24(4) (× 1)
Cu_B–Cl		2.759 (× 1) 2.831 (× 1)	2.90(1) (× 1) 2.95(1) (× 1)

[a] Metal–chloride and metal–oxygen(hydroxide) distances in Å.

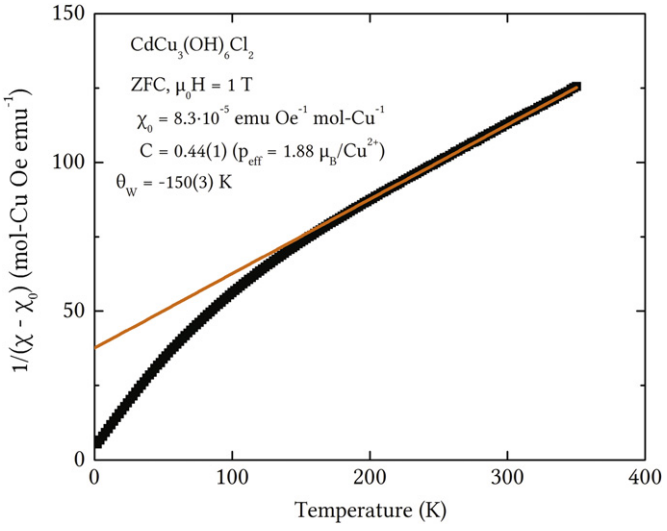

Fig. 4. Inverse magnetic susceptibility of $CdCu_3(OH)_6Cl_2$ is consistent with strong antiferromagnetic interactions within the Cu^{2+} kagomé layers, $\theta W = -150$ K, but there is no cusp that would indicate a transition to a long range ordered antiferromagnetic state down to $T = 2$ K. Thus $CdCu_3(OH)_6Cl_2$ exhibits geometric magnetic frustration.

$T \sim 200$ K. A fit of the region $T = 280$–350 K gives a Curie constant of 0.44(1) per Cu^{2+} and a Weiss temperature of $\theta_w = -150$ K. The Curie constant yields a $p_{eff} = 1.9\ \mu_B$, as expected for Cu^{2+}. The Weiss temperature is large and negative, implying the existence of strong antiferromagnetic interactions within the Cu^{2+} kagomé layers. As with the related Herbertsmithite materials [6,15], there is no apparent transition to long range magnetic order above $T = 2$ K, even though the magnetic interactions are strong, on the order of ~ 150 K. Thus, despite the different arrangement of cations to form the kagomé layers, $CdCu_3(OH)_6Cl_2$ is still a geometrically frustrated antiferromagnet.

In addition to similarities in magnetic properties, the structure of $CdCu_3(OH)_6Cl_2$, and related hydroxide chlorides, can be understood as being built of a $[(OH)_3Cl]^{4-}$ pseudopolyatomic anion, diagramed in Fig. 5a. Although chlorine is not usually considered capable of hydrogen bonding in molecular species, it is well-known to do so in the solid state [24], and the average O–Cl distance in one of the pseudopolyatomic anions in $CdCu_3(OH)_6Cl_2$ is 2.92 Å, in line with the expected sum of covalent O–H (0.97 Å) and hydrogen-bonding H–Cl (2.2 Å) interactions. As a result, the structural polymorphs of these hydroxide chlorides result from different rotations and tilts of this complex anion, in combination with cations in different resulting 'holes'. As shown in Fig. 5b, the Herbertsmithite [1], $CdCu_3(OH)_6Cl_2$, and Kapellasite [2] structures have the same basic packing of $[(OH)_3Cl]^{4-}$ tetrahedra. Compared to Herbertsmithite, the $[(OH)_3Cl]^{4-}$ anions in $CdCu_3(OH)_6Cl_2$ are tilted along two separate axes (across and into page) in a tick/tock fashion. This accommodates the both the Jahn–Teller distortion of the Cu1 ion and the large size of Cd^{2+}. The cation distribution is also changed to allow Cd^{2+} to go into the larger O_4Cl_2 cavity, resulting in kagomé layers running diagonal to those found in Herbertsmithite. The Kapellasite structure highlights the geometrical flexibility of a pseudopolyatomic anion compared to a traditional polyatomic anion (e.g. sulfate, phosphate, etc.). Kapellasite has cations in different holes within the anion framework, which tends to 'draw up' the $[(OH)_3Cl]^{4-}$ anions. There is sufficient tall/flat flexibility due to the hydrogen bonding that the tetrahedral anions can stay packed in an ideal geometry. The result is a unified view of the origins of the structural variations in this family of layered hydroxide chlorides: size and electronic effects of cations coupled with the structural abilities of the pseudopolyatomic $[(OH)_3Cl]^{4-}$ anion.

5. Conclusions

The structure of the new compound $CdCu_3(OH)_6Cl_2$ and related hydroxide chlorides can be rationalized on the basis of $[(OH)_3Cl]^{4-}$ pseudopolyatomic anions that pack and rotate, in much the same way as do traditional polyatomic ions such as SO_4^{2-} and PO_4^{3-}.

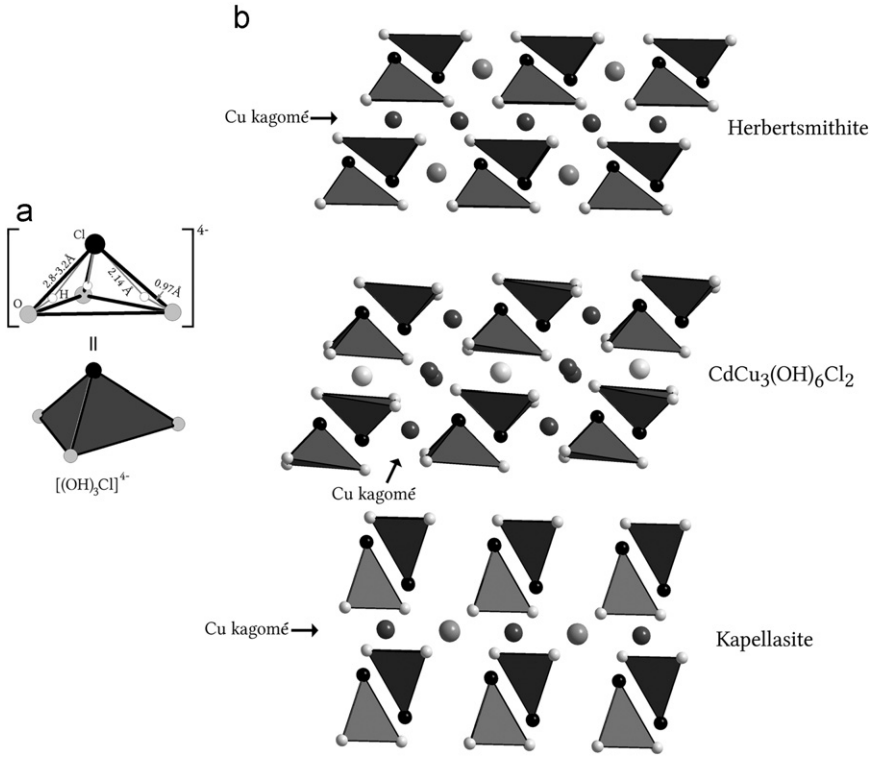

Fig. 5. (a) The $[(OH)_3Cl]^{4-}$ pseudopolyatomic anion. (b) Relationship of the Herbertsmithite, $CdCu_3(OH)_6Cl_2$, and Kapellasite hydroxide chloride structures in terms of the $[(OH)_3Cl]^{4-}$ anion. All three have the same basic packing of $[(OH)_3Cl]^{4-}$ tetrahedra. The first two have cations in the same locations, but there is a rotation and tilt of the $[(OH)_3Cl]^{4-}$ anions in $CdCu_3(OH)_6Cl_2$. In Kapellasite, the cations are in different holes within the anion framework; the geometrical flexibility of the anion is able to accommodate this difference in cation location.

The layered structure contains distorted kagomé layers of magnetic Cu^{2+} ions separated by non-magnetic ions that have strong antiferromagnetic interactions, $\theta_w = -150$ K, but no long range magnetic order down to $T = 2$ K. The large size of the Cd^{2+} ion when compared to Zn^{2+} or Mg^{2+} explains the large difference in the structure compared to the "$ZnCu_3(OH)_6Cl_2$" or "$Mg_xCu_{4-x}(OH)_6Cl_2$" compounds. More generally, we expect the concept of pseudopolyatomic anions to aid the understanding of the wide variety of related hydroxide chlorides that are known, and to aid in the rational design of new hydroxide chlorides with improved physical properties.

Acknowledgments

This work was supported primarily by the MRSEC Program of the NSF under award number DMR 0819762, and YL was supported by the DOE under Grant no. DE-FG02-04ER46134.

References

[1] R.S.W. Braithwaite, K. Mereiter, W.H. Paar, A.M. Clark., Mineral. Mag. 68 (2004) 527–539.
[2] W. Krause, H.J. Bernhardt, R.S.W. Braithwaite, U. Kolitsch, R. Pritchard, Mineral. Mag. 70 (2006) 329–340.
[3] K. Schmetzer, G. Schnorrerkohler, O. Medenbach, Neues Jahrbuch Fur Mineralogie-Monatshefte (1985) 145–154.
[4] E.V. Sokolova, Y.K. Egorovtismenko, Kristallografiya 35 (1990) 995–997.
[5] F.C. Hawthorne, E. Sokolova, Can. Mineral. 40 (2002) 939–946.
[6] M.P. Shores, E.A. Nytko, B.M. Bartlett, D.G. Nocera, J. Am. Chem. Soc. 127 (2005) 13462–13463.
[7] M.A. de Vries, K.V. Kamenev, W.A. Kockelmann, J. Sanchez-Benitez, A. Harrison, Phys. Rev. Lett. 100 (2008) 157205.
[8] R.H. Colman, C. Ritter, A.S. Wills, Chem. Mater. 20 (2008) 6897–6899.
[9] O. Janson, J. Richter, H. Rosner, Phys. Rev. Lett. 101 (2008) 106403.
[10] R.H. Colman, A. Sinclair, A.S. Wills, Chem. Mater. 22 (2010) 5774–5779.
[11] J.S. Helton, K. Matan, M.P. Shores, E.A. Nytko, B.M. Bartlett, Y. Yoshida, Y. Takano, A. Suslov, Y. Qiu, J.H. Chung, D.G. Nocera, Y.S. Lee, Phys. Rev. Lett. 98 (2007) 107204.
[12] A.S. Wills, R.H. Colman, A. Sinclair, Chem. Mater. 23 (2011) 1811–1817.
[13] D. Wulferding, P. Lemmens, P. Scheib, J. Roder, P. Mendels, S.Y. Chu, T.H. Han, Y.S. Lee, Phys. Rev. B 82 (2010) 144412.
[14] T.H. Han, J.S. Helton, S. Chu, A. Prodi, D.K. Singh, C. Mazzoli, P. Muller, D.G. Nocera, Y.S. Lee, Phys. Rev. B 83 (2011) 100402.
[15] S.Y. Chu, T.M. McQueen, R. Chisnell, D.E. Freedman, P. Muller, Y.S. Lee, D.G. Nocera, J. Am. Chem. Soc. 132 (2010) 5570–5571.
[16] D.E. Freedman, T.H. Han, A. Prodi, P. Muller, Q. Huang, Y.S. Chen, S.M. Webb, Y.S. Lee, T.M. McQueen, D.G. Nocera, J. Am. Chem. Soc. 132 (2010) 16185–16190.
[17] M.A. de Vries, A. Harrison, Nature 468 (2010) 908–909.
[18] R.D. Shannon, C.T. Prewitt, Acta Crystallogr. Sect B—Struct. Crystallogr. Crys. Chem. B 25 (1969) 925.
[19] T.M. McQueen, P.W. Stephens, Q. Huang, T. Klimczuk, F. Ronning, R.J. Cava, Phys. Rev. Lett. 101 (2008) 166402.
[20] R.E. Schaak, T. Klimczuk, M.L. Foo, R.J. Cava, Nature 424 (2003) 527–529.
[21] X.G. Zheng, T. Kawae, Y. Kashitani, C.S. Li, N. Tateiwa, K. Takeda, H. Yamada, C.N. Xu, Y. Ren, Phys. Rev. B 71 (2005) 052409.
[22] W.C. Hamilton, Acta Crystallogr. 18 (1965) 502.
[23] L. Walterle, D. Groult, Comptes Rendus Hebdomadaires Des Seances De L Academie Des Sciences Serie C 270 (1970) 1966.
[24] T. Steiner, Ange. Chemie—Int. Ed. 41 (2002) 48–76.